

## Characterization of a GaN Epilayer with a LT-AlN Interlayer on Si(111) by HRXRD and RBS/Channeling

Bin-feng Ding\*

*Department of Physics and Electronic Information,  
Langfang Teachers College, Langfang 065000, China*  
(Received June 2, 2011; Revised July 9, 2011)

A hexagonal GaN layer with a LT-AlN (low temperature) interlayer grown on Si(111) by the metal-organic chemical vapour deposition (MOCVD) method was characterized by high resolution X-ray diffraction (HRXRD) and Rutherford backscattering (RBS)/channeling. The crystal quality of the film is very good with  $\chi_{\min} = 2.5\%$ . According to the results of the XRD  $\omega$ -scan, a big mismatch between the GaN epilayer and the substrate Si(111) was determined. The elastic strains in the perpendicular and parallel directions were calculated to be  $-0.10\%$  and  $0.13\%$  respectively by  $\theta - 2\theta$  scans of the GaN(0002) and GaN(11 $\bar{2}$ 2) diffractions. By the angular scan around an off-normal ( $1\bar{2}13$ ) axis in the (10 $\bar{1}0$ ) plane of the GaN layer, the tetragonal distortion  $e_T$ , which is caused by the elastic strain, was determined to be  $0.18\%$  near the surface, indicating a tensile strain in the parallel direction ( $e^{\parallel} > 0$ ), which results in a compressive strain in the perpendicular direction ( $e^{\perp} < 0$ ) due to the elastic properties of the epilayer. This result coincides perfectly with that from XRD. The elastic strain of the GaN epilayer below the AlN interlayer releases more quickly than that above the AlN interlayer, which will avoid film cracks efficiently and improve the crystal quality of the GaN film remarkably.

PACS numbers: 82.33.Ya, 82.80.Yc, 61.05.cp, 68.35.Gy

### I. INTRODUCTION

The III-nitride family is one of the most promising optoelectronic materials [1, 2]. The bandgap of (In, Ga, Al)N and their alloys can cover the wavelength from the red to the deep ultraviolet. Due to their special optical and electrical properties, III-nitrides are being used widely in visible light emitters and high-temperature/high power electronics; some of them have been commercialized.

Normally, GaN, InGaN, and AlGaN films are grown on sapphire using metal-organic chemical vapour deposition (MOCVD). Recently the crystal quality of GaN on Si(111) improved greatly [3]. Compared with a sapphire substrate, Si substrate has some advantages. First, high quality Si substrates are available in large sizes (300 mm) at a relatively low cost. Another important consideration is the integration of the microelectronics and optoelectronics. For many years, the low emitting efficiency of Si made it impossible to integrate microelectronics and optoelectronics. The success in growth of GaN on the Si substrate will facilitate the integration. But the large difference in the lattice constants of GaN ( $a_{\text{GaN}} = 0.3189$  nm) and Si ( $a_{\text{Si}(111)} = 0.38403$  nm) results in a large lattice mismatch ( $-16.9\%$ ). What is more, the in-plane thermal expansion coefficients of GaN and Si are  $5.59 \times 10^{-6}/\text{K}$  and  $3.77 \times 10^{-6}/\text{K}$  respectively, which leads to a large tensile stress and

cracks in thick GaN layers during cooling from the growth temperature (1100 °C~1200 °C) to room temperature. The relaxation of the stress results in a high density of dislocation of  $\sim 10^{10}/\text{cm}^2$ . The residual stress can affect the bandgap of GaN. Using low-temperature (500 °C~600 °C) AlN (LT-AlN) interlayers is an effective method to reduce the tensile stress and cracks in thick GaN layers on Si [4–6].

In this work, a high quality GaN layer with a LT-AlN interlayer on Si(111) was characterized by high resolution XRD and RBS/C. With the depth resolution of RBS/C, the strain status below and above the LT-AlN interlayer were compared.

## II. EXPERIMENTS

The GaN sample was grown in a horizontal type low pressure (76 Torr) metal-organic chemical vapour deposition system. The GaN was grown on Si(111) at 1120 °C. When the thickness of the GaN epilayer reached about 0.5  $\mu\text{m}$ , the temperature was decreased to 600 °C to grow a LT-AlN interlayer, and then the temperature was raised to 1120 °C again to continue the GaN growth process. The precursors for AlN and GaN were trimethylaluminum (TMAI), ammonia ( $\text{NH}_3$ ) and trimethylgallium (TMGa), ammonia ( $\text{NH}_3$ ) respectively.  $\text{N}_2$  was used as a carrier gas during the growth.

X-ray diffraction is a non-destructive method of investigating the structural properties of film material [7]. High Resolution diffraction is particularly suited to the examination of materials with high crystalline perfection, such as single crystals and epitaxial layers. For this work, a Bruker D8-discover system, equipped with a Ge(220) monochromator, was used. A monochromatic Cu  $K\alpha_1$  ray ( $\lambda = 0.15406 \text{ nm}$ ) was used as the incident light. Three different X-ray diffraction measurements were taken: (1) rocking curve scans of GaN(0002) and Si(111) reflections at twelve different azimuth angles, respectively, and (2) the conventional  $\theta - 2\theta$  scans normal to the epilayer plane at  $0^\circ$  and  $180^\circ$  azimuth angles. (3) The  $\theta - 2\theta$  scans of GaN( $11\bar{2}2$ ) reflection at two azimuth angles were also measured at an asymmetric mode.

Rutherford backscattering/channeling (RBS/C) is a powerful technique to characterize the composition, thickness, and crystal quality of the thin film directly and nondestructively. When the ion beam is directed along a high-symmetry crystal direction, it has less chance to collide with the host atoms. This will result in channeling, and consequently the backscattering events in a film of good crystalline quality will be significantly reduced compared with the probability for the ion beam directed in a random (non-channeled) direction. The ratio of the backscattering yield along the  $\langle 0001 \rangle$  axis to that from the random direction in the near surface region, normally defined as  $\chi_{\text{min}}$ , can be used to quantify the crystalline quality. Especially,  $\chi_{\text{min}}$  is sensitive to the density of point defects.  $\chi_{\text{min}}$  is usually given as a percentage: a value of 1–2% indicates perfect crystalline quality and 100% an amorphous or polycrystalline material. What's more, the angular scan around an off-normal axis can determine the tetragonal distortion induced by the elastic strain in the epilayer. Then the strain calculated by the RBS/channeling and XRD can confirm each other. On the other hand, the method of RBS/C is depth sensitive and can be used to

determine the strain in the film as a function of depth, which is impossible for normal XRD. In this study, a collimated 1.57 MeV He<sup>+</sup> beam was used. The sample was mounted on a high precision (0.01) three-axis goniometer in a vacuum chamber. The backscattered He<sup>+</sup> ions were collected by an Au-Si barrier detector with an energy resolution of 15 keV located at 170. The off-normal axis  $\langle 1\bar{2}13 \rangle$  is chosen to study the elastic strain related tetragonal distortion of the GaN epilayer. For unstrained GaN, the angle between the  $\langle 0001 \rangle$  axis and the off-normal  $\langle 1\bar{2}13 \rangle$  axis is 31.59 in the  $(10\bar{1}0)$  plane calculated by  $\Phi_b = \tan^{-1}(a_b/c_b)$ , where  $a_b$  and  $c_b$  are the lattice constants of unstrained GaN. The sample is tilted step by step in the  $(10\bar{1}0)$  plane and around the  $\langle 1\bar{2}13 \rangle$  axis direction from  $-2.00$  to  $+2.00$  with a step size of 0.20 and thus 21 RBS spectra are obtained [8]. Then 21 RBS spectra around the  $\langle 0001 \rangle$  axis in the  $(10\bar{1}0)$  plane are measured correspondingly. The depth information can be deduced from the different energy windows in the RBS angular scan spectra of the  $\langle 0001 \rangle$  axis and the  $\langle 1\bar{2}13 \rangle$  axis.

### III. RESULTS AND DISCUSSIONS

#### III-1. The tilt between GaN and Si

Generally there is a little deflective angle between the orientation of the Si(111) and the surface in the Si(111) wafer. As a result, a tilt will occur between GaN(0001) and Si(111). XRD is an effective method to obtain this tilt by measuring the true peak separation between the substrate and epilayer peaks of the rocking curve at different rotary angles. The tilt angle  $\beta$  can be calculated by the following equation  $\beta = \omega_{\text{GaN}} - \omega_{\text{Si}} - \Delta\omega$ , where  $\Delta\omega$  is the theoretical separation of  $\omega$  angles ( $\omega = \theta$ ) of GaN(0002) and Si(111) reflections [9]. The theoretical Bragg angles of GaN(0002) and Si(111) reflections are  $17.285^\circ$  and  $14.221^\circ$  respectively, so  $\Delta\omega = \theta_B^{\text{GaN}(0002)} - \theta_B^{\text{Si}(111)} = 17.285^\circ - 14.221^\circ = 3.064^\circ$ .  $\omega_{\text{GaN}}$  and  $\omega_{\text{Si}}$  are the values of experimental Bragg angles which can be obtained by Gauss Function Fit of the rocking curve scan of GaN(0002) and Si(111) reflections with the fixed  $2\theta_b^{\text{GaN}(0002)} = 34.57^\circ$  and  $2\theta_b^{\text{Si}(111)} = 28.442^\circ$  respectively. Fig. 1 is the rocking curve of GaN(0002) reflection at 0 azimuth angle. The calculated tilt angle  $\beta$  is dependent on the azimuth angle. The maximum is the best approach to the real tilt angle. In our work, twelve measurements were made, one at each 30 rotation about the surface normal (Table I), to accurately determine the tilt between the GaN epilayer and Si(111) substrate. Fig. 2 shows the dependence of the  $\omega$  angle on the azimuth angle. The solid lines are the Gauss fitting results. The maximal separation between  $\omega_{\text{GaN}}$  and  $\omega_{\text{Si}}$  is  $14.428^\circ - 9.908^\circ = 4.520^\circ$  by Gauss Fit. So the tilt angle between the GaN epilayer and Si(111) can be calculated to be  $\beta = \omega_{\text{GaN}} - \omega_{\text{Si}} - \Delta\omega = 14.428^\circ - 9.908^\circ - 3.064^\circ = 1.456^\circ$ . However, the tilt angle between the GaN(0001) and Si(111) obviously cannot reduce the mismatch between the GaN and Si, which is calculated by the following equation:  $f = \frac{a_{\text{GaN}} - a_{\text{Si}(111)}}{a_{\text{Si}(111)}} \cdot \cos \beta = -16.89\%$ .

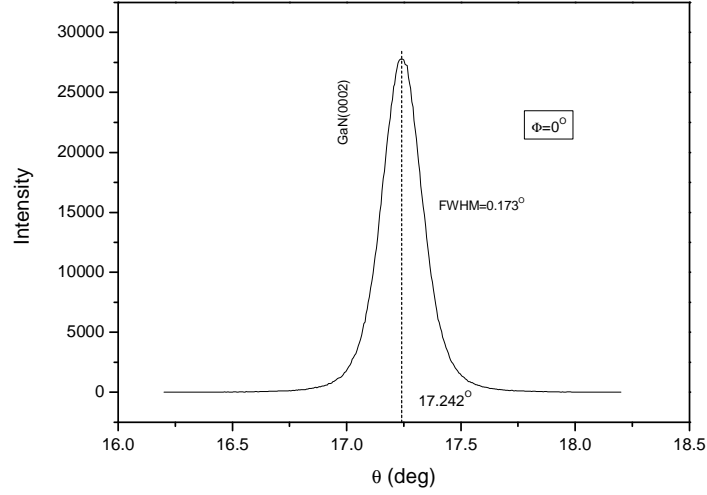


FIG. 1: Rocking curve of GaN(0002) at 0 azimuth angle of the sample.

TABLE I: The data of rocking curve scan between GaN(0002) and Si(111) at each 30° rotation.

$\Phi$ (deg.)	-180	-150	-120	-90	-60	-30
GaN (0002) (deg.)	17.199	15.811	14.781	14.428	14.865	15.898
Si(111) (deg.)	14.123	12.009	10.463	9.9076	10.489	12.046
$\Phi$ (deg.)	0	30	60	90	120	150
GaN (0002) (deg.)	17.242	18.606	19.656	20.049	19.646	18.591
Si(111) (deg.)	14.157	16.270	17.816	18.380	17.796	16.241

### III-2. Residual strain and tetragonal distortion in GaN

High resolution XRD is an effective method for determining the lattice constants ( $a$  and  $c$ ) of thin films combining a symmetric and an asymmetric  $\theta - 2\theta$  scan (Fig. 3). Fig. 3 shows a symmetric and an asymmetric  $\theta - 2\theta$  scan of X-ray diffraction from GaN(0002) and GaN(11 $\bar{2}$ 2) reflections. Taking the peak of the Si(111) substrate as a reference, the Bragg angle of GaN(0002) can be determined accurately. According to the equation of  $2d \sin(\theta) = \lambda$ , we can get the lattice constant  $c_{\text{epi}}$  of GaN to be 0.5180 nm, The  $\theta - 2\theta$  scan of GaN(11 $\bar{2}$ 2) reflection was chosen to determine the lattice constant  $a_{\text{epi}}$ . Combining the value of  $c_{\text{epi}}$  and the following equation  $d_{hkl} = \frac{1}{\sqrt{\frac{4}{3}(\frac{h^2+k^2}{a^2} + (\frac{l^2}{c^2})}}$ , the lattice constant  $a_{\text{epi}}$  is calculated to be 0.3193 nm. Then the elastic strains in the perpendicular and parallel directions can be calculated by the following formulas  $e^{\parallel} = a_{\text{epi}} - a_0/a_0$ ,  $e^{\perp} = (c_{\text{epi}} - c_0)/c_0$ , where  $a_0$  and  $c_0$

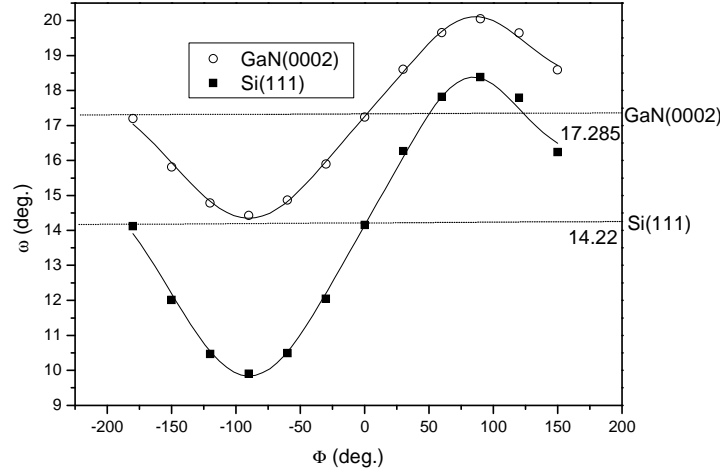


FIG. 2: The azimuth angle dependence of the  $\omega$  angle of the sample. The solid lines are the Gauss fitting result.

are the lattice constants of block materials.  $e^{\parallel} = \frac{0.3193-0.3189}{0.3189} = 0.13\% > 0$  means that the epilayer is under tensile strain in the parallel direction, and  $e^{\perp} = \frac{0.5180-0.5185}{0.5185} = -0.10\% < 0$  means a compressive strain in the perpendicular direction. Table II is the lattice constant of the epitaxial layer ( $a_{\text{epi}}$ ,  $c_{\text{epi}}$ ), the critical epilayer thickness and the degree of epilayer bulging by XRD and RBS/C (combining Fig. 4(a) and Fig. 4(b)), from Table II we can see that the degree of epilayer bulging decreases with an AlN interlayer, this certifies that the GaN epilayer is high crystal quality; it will avoid the GaN epilayer cracks efficiently.

TABLE II: The lattice constant of the epitaxial layer, the critical epilayer thickness and the degree of epilayer bulging.

The epilayer	Lattice constant (nm)				epilayer thickness (nm)		The degree of bulging ( $\text{K}^{-1}$ )		
	$a_0$	$a_{\text{epi}}$	$c_0$	$c_{\text{epi}}$	GaN	AlN	GaN	$\Delta a/a_0/300$	$\Delta a/a_0/300$
GaN	0.3189	0.3193	0.5185	0.5180	455	20	557	$5.59 \times 10^{-6}$	$4.18 \times 10^{-6}$

Fig. 4(a) shows the random(O),  $\langle 0001 \rangle$  aligned( $\star$ ), and the simulated (solid line) spectra of the sample. The label of Ga shows the energy of the  $\text{He}^+$  backscattered from the Ga atoms at the surface and the FWHM (full width at half maximum) of backscattered spectrum from Ga atoms indicates the thickness of the GaN film. The pit on the backscattered spectrum indicates the depth and thickness of the AlN interlayer. The  $\langle 0001 \rangle$  aligned spectrum shows that the GaN film grown on Si(111) has minimum yield  $\chi_{\text{min}} = 2.5\%$ , indicating that the GaN epilayer has a very good crystalline quality. A simulation (solid line)

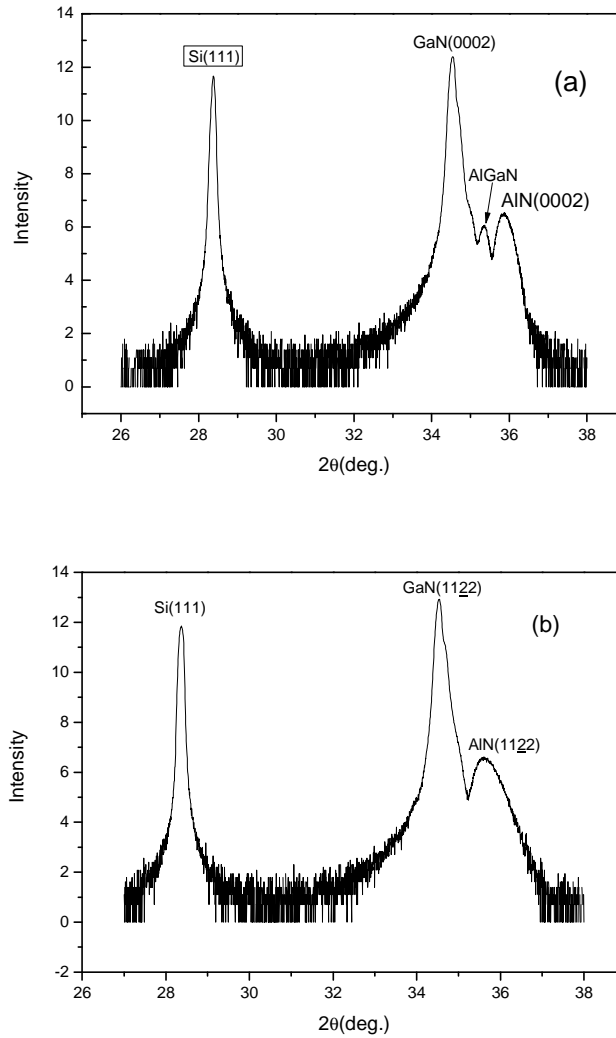


FIG. 3: Symmetric and asymmetric  $\theta - 2\theta$  scan of X-ray diffraction. (a) From GaN(0002) and Si(111) of the sample. (b) From GaN(11 $\bar{2}$ 2) and Si(111) of the sample.

of the random spectrum can be given using the RUMP program [10]. Then the structure of the epilayer can be given to be 455 nm GaN, 20 nm AlN, and 557 nm GaN from the substrate to the surface (Fig. 4(b) & Table II).

Fig. 5 shows the aligned spectrum ( $\star$ ) along the off-normal  $\langle 1\bar{2}13 \rangle$  axis, the random spectrum (O), and the simulated spectrum (solid line). The  $\chi_{\min}$  along the  $\langle 1\bar{2}13 \rangle$  axis was calculated to be 3.4%, higher than that of the  $\langle 0001 \rangle$  axis because of the higher index of this axis. The dechanneling rate of this aligned spectrum is much larger than that of the  $\langle 0001 \rangle$  aligned spectrum because the dechanneling of the ion beam along the  $\langle 1\bar{2}13 \rangle$  axis

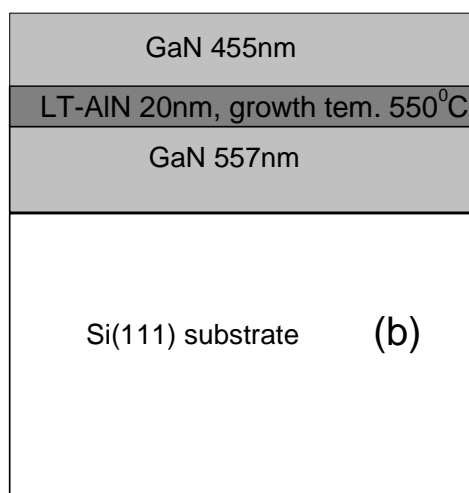
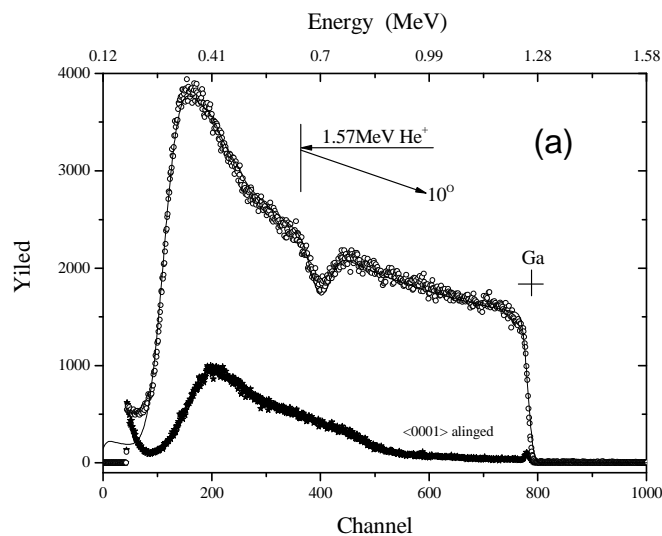


FIG. 4: (a) Random (O),  $\langle 0001 \rangle$  axis aligned ( $\star$ ), and simulated (solid line) RBS spectra of the sample. (b) The growth structure of the sample by RBS/C experiment.

is higher than that along the  $\langle 0001 \rangle$  axis. The tetragonal distortion induced by the elastic strain in different depths of the epilayer can be determined by choosing different energy windows of the 21 RBS spectra around the  $\langle 1\bar{2}13 \rangle$  axis. 9 angular scans around the  $\langle 1\bar{2}13 \rangle$  axis were obtained, and each one related to a specific depth region defined by the energy windows, which are shown in Fig. 5 and Table III. As an example, the angular scan around the  $\langle 1\bar{2}13 \rangle$  axis corresponding to the energy window 8 in the near surface region ( $-120$

nm) is shown on the right-hand side in Fig. 6, and an angular scan in the  $(10\bar{1}0)$  plane around the  $\langle 0001 \rangle$  axis is shown on the left-hand side. Gauss Function Fits (solid line) are used to accurately determine the position of the dips (dotted line) respectively. The inset in Fig. 6 shows the sketch map that the direction of the  $\langle 1\bar{2}13 \rangle$  axis in the  $(10\bar{1}0)$  plane (which also contains the  $\langle 0001 \rangle$  and  $\langle 11\bar{2}0 \rangle$  axes) will be changed when there is tetragonal distortion. The angle between the  $\langle 0001 \rangle$  axis and  $\langle 1\bar{2}13 \rangle$  axis can be calculated from Fig. 6,  $\Phi_{\text{epi}} = \tan^{-1}(a_{\text{epi}}/c_{\text{epi}}) = 29.327^\circ - (-2.309^\circ) = 31.636^\circ$ , where  $a_{\text{epi}}$  and  $c_{\text{epi}}$  are the lattice constants of the epilayer. So,  $\Delta\Phi = \Phi_{\text{epi}} - \Phi_b = 31.636^\circ - 31.59^\circ = 0.046^\circ$  and the tetragonal distortion  $e_T = e^{\parallel} - e^{\perp} = \Delta\Phi/(\sin\Phi \cos\Phi) = 0.18\%$  can be determined at the depth of  $-120$  nm.  $e_T > 0$  means that the epilayer is under tensile strain in the parallel direction ( $e^{\parallel} > 0$ ), which results in a compressive strain in the perpendicular direction ( $e^{\perp} < 0$ ) due to the elastic properties of the epilayer, in agreement with the results from XRD. Whether the  $e_T$  value is positive or negative depends on whether the lattice mismatch is negative or positive, respectively [11]. From Fig. 7 by Table III, we can see that the elastic strain of the epilayer before the AlN interlayer releases more quickly than after the interlayer with the thickness increasing, and has a break at the AlN interlayer. This shows that the AlN interlayer has a great influence on the strain of the epilayer. The  $e_T$  value should decrease along the thickness of the epilayer [8]. In the SEM micrograph, no obvious cracks were observed at the surface of the sample, as shown in Fig. 8.

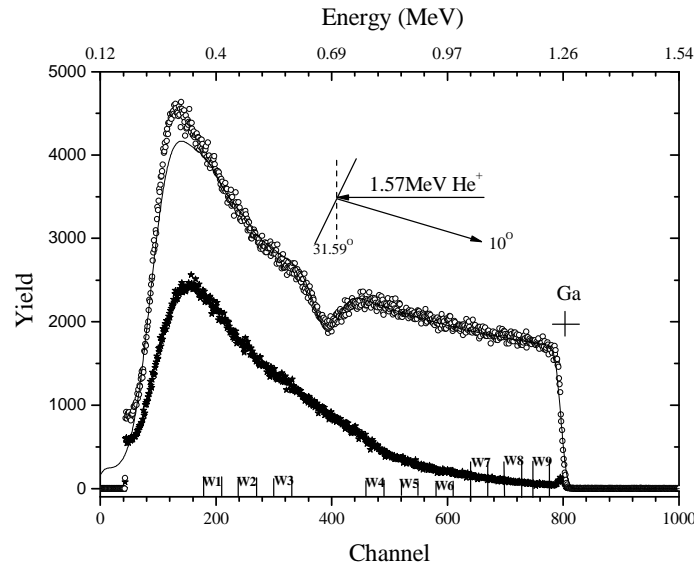


FIG. 5: Random (O),  $\langle 1\bar{2}13 \rangle$  axis aligned ( $\star$ ), and simulated (solid line) RBS spectra of the sample.



TABLE III: The different depths corresponded to the different energy windows and the tetragonal distortion( $e_T$ ).

Energy Window	1	2	3	4	5	6	7	8	9
Start channel	180	240	300	460	520	580	640	700	745
End channel	210	270	330	490	550	610	670	730	775
Depth (nm)	-800	-700	-600	-520	-420	-320	-220	-120	-60
$e_T$ (%)	0.321	0.289	0.27	0.17	0.21	0.19	0.181	0.179	0.169
Error angle (%)	0.01605	0.01445	0.0135	0.0085	0.0105	0.0095	0.00905	0.00895	0.00845

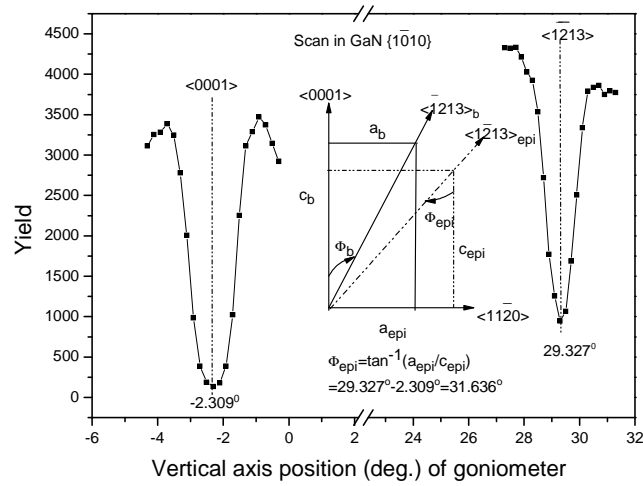


FIG. 6: Angular scans along the  $\langle 0001 \rangle$  axis and the  $\langle 1\bar{2}13 \rangle$  axis in the  $(10\bar{1}0)$  plane.

#### IV. CONCLUSIONS

The structure and strain properties of a high quality GaN epilayer on Si(111) was studied. HRXRD is a powerful and non-destructive method which can be used to calculate the tilt angle between the GaN epilayer and Si substrate, the average lattice constants, and the elastic strain of the GaN epilayer. RBS/channeling spectroscopy can give the structure, and the depth dependence of tetragonal distortion induced by the strain of the epilayer. The LT-AlN interlayer can reduce the strain relaxation; this could be helpful to avoid film cracks, which can be evidenced by SEM directly.

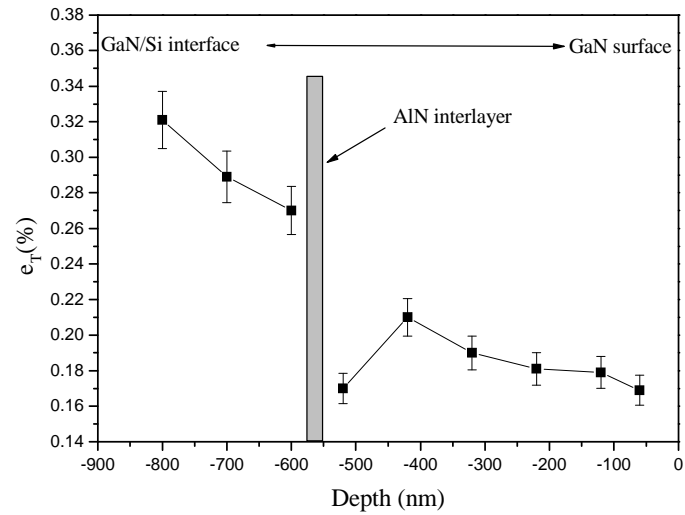


FIG. 7: The depth dependence of the tetragonal distortion measured by RBS/channeling.

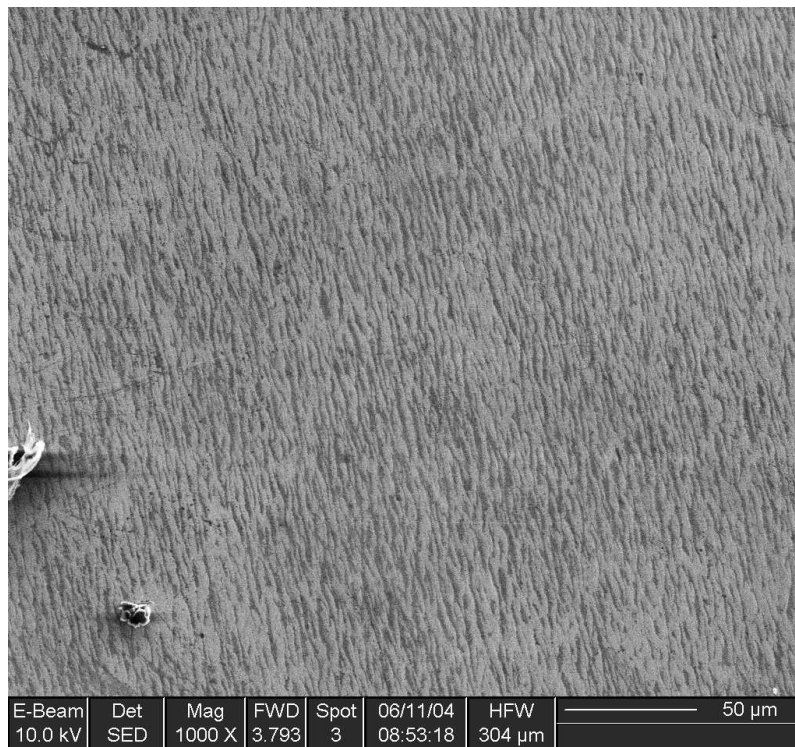


FIG. 8: The SEM micrograph of the surface.

## Acknowledgements

The research was supported by the National Natural Science Foundation of China under the grant No.50802041 & No. 50872050 and the 2011 Key Project of the Langfang Teachers College under the grant No.LSZZ201101.

## References

- \* Electronic address: [ding\\_binfeng@126.com](mailto:ding_binfeng@126.com)
- [1] S. Nakamura, S. J. Pearton, and G. Fasol, *The blue laser diode*, 2nd ed. (Germany, Springer, 2000), Chap. 7.
  - [2] F. A. Ponce and D. P. Bour, *Nature* **386**, 351 (1997).
  - [3] A. Krost and A. Dadgar, *Mat. Sci. & Eng. B* **93**, 77 (2002).
  - [4] H. Amano *et al.*, *Jpn. J. Appl. Phys.* **37**, L1540 (1998).
  - [5] M. Iwaya *et al.*, *Applied Surface Science* **405**, 59 (2000).
  - [6] K. E. Waldrip *et al.*, *Appl. Phys. Lett.* **78**, 3205 (2001).
  - [7] Z. C. Feng *et al.*, *Thin Solid Films* **409**, 15 (2002).
  - [8] M. F. Wu *et al.*, *Appl. Phys. Lett.* **80**, 4130 (2002).
  - [9] S. Q. Zhou, A. Vantomme, B. S. Zhang, H. Yang, and M. F. Wu, *Appl. Phys. Lett.* **86**, 081912 (2005).
  - [10] L. R. Doolittle, *Nucl. Instrum. Methods. Phys. Res. B.* **9**, 344 (1985).
  - [11] M. F. Wu *et al.*, *Vac. Sci. Technol. B* **17**, 1502 (1999).